Building extraction at the State Research Institute of Aviation Systems (GosNIIAS)

S.U. Zheltov, A.V. Sibiryakov & A.E. Bibitchev
State Research Institute of Aviation Systems (GosNIIAS), Moscow, Russia

ABSTRACT: Current GosNIIAS research towards technology of 3D-site model generation is briefly summarized. Most challenging part of the technology that is automatic and semi-automatic methods of man-made object extraction from aerial images is described. The satisfactory results are obtained at extraction of serial type buildings and objects with simple geometry. The proposed automatic approach consists of digital elevation model based building detection, straight line grouping and precise 3D reconstruction through correlation in object space. Semi-automatic approach uses key points defined by the user to extract building regions and Hough transform based detection of contours.

1 INTRODUCTION

The modern situation in Russia in the field of geo-informational support of decision making is characterized by lack of regular high fidelity original data on the one hand and the predominance of low cost computer maintenance on the other hand. This paper is devoted to elements of the technology developed in GosNIIAS aimed at using of various data sources on PC-level computers to provide 3D site modeling for a wide variety of applications, from military mission planning, mission rehearsal and reconnaissance data analysis to urban and landscape planning, transport flow planning and the virtual tourism (Zheltov et al. 1997).

Quickly growing field of planning and decision support systems require effective tools to operate with spatial distributed information. The modern virtual GIS using 3D representation of the real territories are designed to decide most problems. Nowadays because of difficulties to have a high detailed 3D digital world model due to limited computer possibilities the following way is realized in GosNIIAS. The GIS data (electronic maps) provide the stationary base with rather large step of the grid and artificial (but nature similar) textures. The space photos (especially made by the topographical camera TK-350 and camera of the high resolution KVR-1000) are the sources of more precise models with natural grey-scale textures. The model of area in the vicinity of most interesting places can be received only by means of aerial photographs or video data processing. The accuracy of such model can achieve about several decimeters both in height and plan.

The technology of 3D-site model generation technology includes:

- photogrammetric and computer vision based processing of images to obtain digital surface and terrain models (DSM and DTM);
- DTM generation from GIS data;
- generation of terrain surface textures;
- automatic and semi-automatic man-made object extraction;
- transformation of these 3D models to standard formats used by well-known systems of 3D objects and scenes construction.

The best sources for DSM generation are satellite and aerial photos. Satellite imagery provides the possibility to obtain original information about large earth areas. For example, one im-

age obtained by Russian TK-350 camera covers the 200 X 300 km area with 10 m resolution. These images are very good for DTM generation on large areas because they have 60% stereoscopic overlap and adequate resolution. Aerial photos have better resolution and less covered area. This data may be used for generation of DTM of small earth regions (approximately 2 X 2 km for one stereo pair and more for the block of photos). It is rational to build these high fidelity DTMs for some significant or "hot" areas. In some cases it is impossible to obtain latest satellite or aerial photos of good quality because of weather conditions. It forces to use GIS data only. Usually GIS data has rather long updating period and relative validity. So it is justified to use this data for models of very large territories with rather big DTM grid step (200 m and more) or in absence of more precise data.

The same source data we use for terrain texture map generation. But in this case there are more wide variety of satellite images. For example, the monoscopic images obtained by Russian KVR-1000 camera (40 X 160 km covered area for one image with 2 m resolution) provide good (aerial like) grayscale terrain textures. So, 7 photos of KVR-1000 approximately cover the same territory as one photo of TK-350. Also we can use satellite images obtained in various spectra or video data. The use of digital topographic map as texture is allowable in some special cases but the most applications need to modify it. We consider that the combination of the elevation representation in green-brown palette (like on physical maps) with some nature like textures and the hydrographic and road nets in some conventional colors is the most appropriate for the wide range of applications.

Satellite images have not enough resolution to reconstruct models of separate objects located on terrain surface. So aerial photos and GIS data at the same scale are the sources for this operation. In many practical cases to render the 3D object models we can use simple coloring with limited number of colors or the standard textures from the specially prepared library. To provide the photorealistic rendering as shown in Figure 1, that in high extent improves human perception of the scene, we should use real true color object textures prepared from ordinary onground photos.

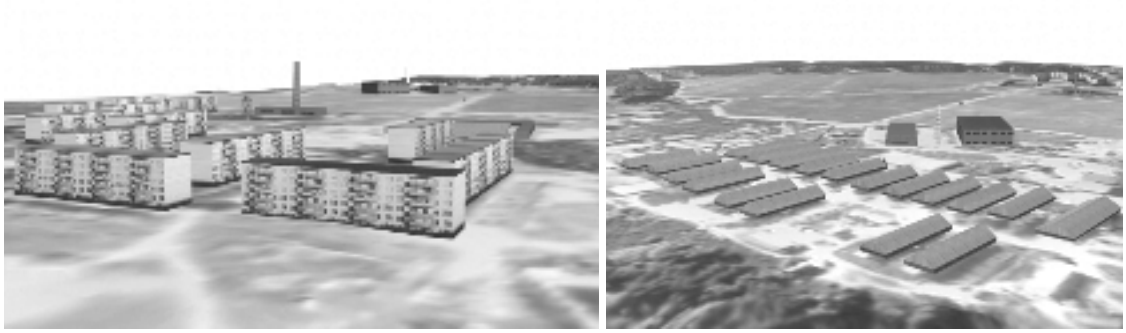

Figure 1. Typical 3D site models with automatically extracted rectangular buildings.

This paper basically concerns our approach to man-made object extraction, because it is the most interesting part of the technology, and because it is one of hardest problem which have no general solution today. The problem of extraction and three-dimensional reconstruction of serial type buildings in a stereopair of large-scale grayscale aerial images is considered. The serial type buildings in most cases satisfy to the following requirements:

- close to the rectangular form of the base;
- verticality of walls;
- absence of niches, arches etc. (i.e. they can be presented at buildings, but constructed 3D-model will not include them);
- have flat or ridge roof which hanging over walls of buildings can be neglected.

2 BUILDING DETECTION

Automatic building extraction consists of detection, grouping and analysis of building contours. For reduction of computational time the areas of interest are detected, in which searching of building contours is performed.

Let there is a not smoothed DSM of considered area obtained by correlation methods with grid size less minimum size of buildings. In this case buildings are presented at the DSM as blobs. Using grayscale morphology one can obtain a DSM with blobs removed. For this purpose the method described in (Eckstein 1996, Haala & Hahn 1995) is used. It consists in application of morphological closing to the DSM image (Fig. 2b). Selection of the structuring element is based on minimum size of a building. In presence of height outliers on an initial rough DSM dual rank filtering is used instead of morphological closing. The areas of interest (Fig. 2c) are obtained by a subtraction of a filtered DSM from an initial DSM. We do not analyze the shape of areas for building hypotheses generation, as the areas can distorted by neighboring trees. Instead we use the areas for fast searching of building features. Obtained areas are sampled by grid size less than minimum size of a building and spatial search table is created (Fig. 2d). Each cell of the table points to the list of building features lying in appropriate image region. This table considerably reduces time of features grouping due to fast access to the close features.

For convenience when working with original images, we create a Digital Elevation Model (DEM) in image coordinates, i.e. for each pixel (i,j) of an image there is an appropriate value of a height H_{ij} on the terrain (Fig. 2a,b). If there is a DSM created in geodesic coordinates it is transformed to the necessary form with the help of photogrammetric collinearity equations and bilinear interpolation.

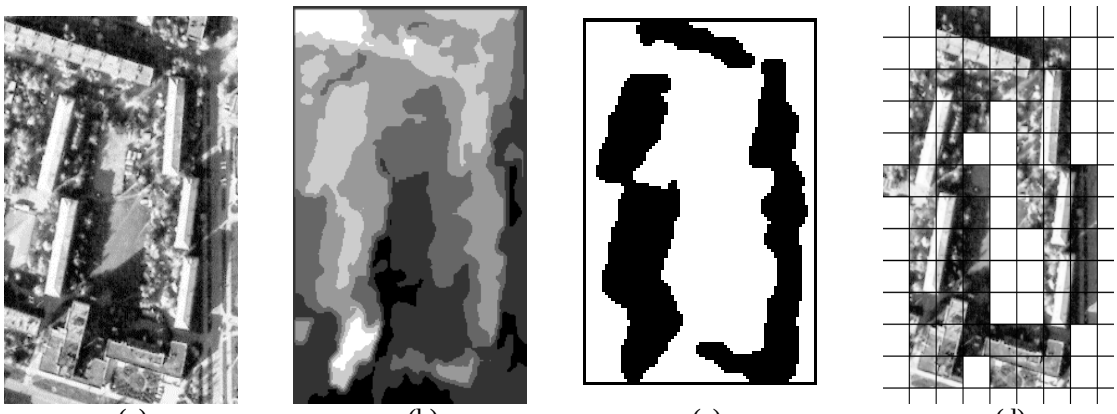

(a) (b) (c) (d)

Figure 2. Illustration for the building detection method. (a) Fragment of the test image (left image of a stereopair); (b) DEM for the test image; (c) Result of dual rank filtering; (d) Spatial search table.

3 MODEL-BASED BUILDING EXTRACTION

In suggested approach straight lines are considered as main features of buildings. For the straight line extraction the method proposed by (Burns et al. 1986) is used, in which edge pixels are first determined by convolution with two 2x2 masks. Then pixels are grouped into line-support regions of a similar gradient orientation. The straight lines (Fig. 3a) are determined by intersection of two planes: first one represents a planar approximation of an intensity surface in the line-support region, second one is a horizontal plane representing an average intensity in the region. For each linear segment attributes shown in Table 1 are stored.

Under linear segments several basic operations and perceptual relations shown in Tables 2,3 are defined, which are used to construct more complex models (see Table 4).

The workflow of the extraction algorithm is illustrated by Figure 3. Two collinear segments are considered to be one long segment, if minimal distance between their endpoints is less than some threshold (Fig. 3b). Further, several collinear segments are considered to be one long

segment, if they are parallel to another segment with overlapping more than some threshold (Fig. 3c,d). Two parallel segments form a parallel pair, if they are overlapped each other and the distance between them is more than a minimal building side (Fig. 3e). A parallel pair forms an U-structure, if there exists a segments l_3 , so that l_1,l_2,l_3 form together an U-shape (Fig. 3f). Two U-structures (l_1,l_2,l_3) and (l_1,l_2,l_4) form a rectangle if l_3 and l_4 lie near the opposite end points of l_1 (Fig. 3g). A rectangle (l_1,l_2,l_3,l_4) forms a ridge if there exists a segment l_5 which is parallel to l_1 and l_2 with overlapping more than a some threshold and it lies within the rectangle (Fig. 3h).

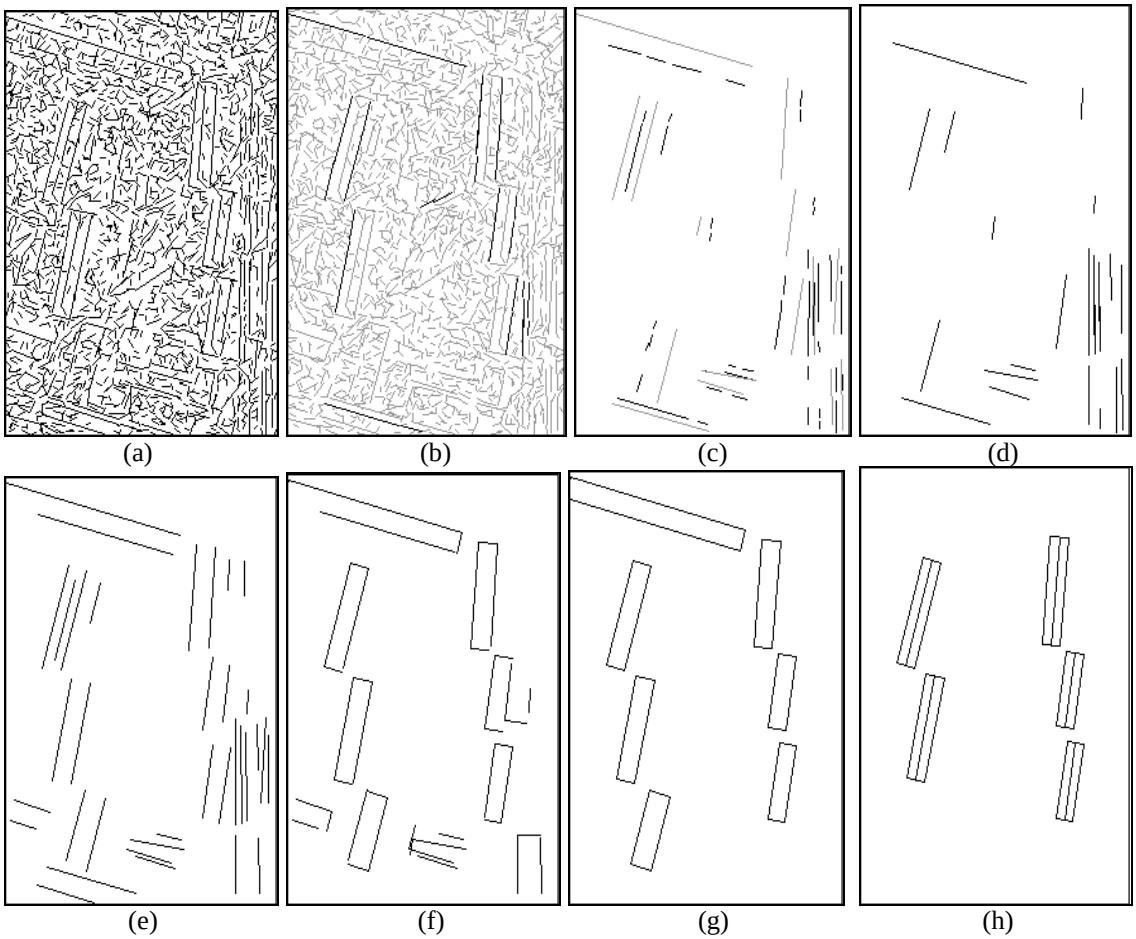

Figure 3. Automatic building extraction. (a) Extracted linear segments; (b) Long segments (shown as black); (c) Searching of long segments by parallelism relation (basic segment is shown as gray, collinear segments parallel to it shown as black); (d) Long segments formed by parallelism relation; (e) Parallel pairs; (f) U-structures; (g) Rectangles; (h) Ridges.

Table 1. Extracted attributes for each linear segment *l*.

Attribute	Label
End points	$(x_1^l, y_1^l), (x_2^l, y_2^l)$
Length	L^l
Normalized parameters of the line equation	a^l, b^l, c^l *
Angle between the line and a horizontal axis	α^l

* $(a^l)^2 + (b^l)^2 = 1$

Table 2. Operations on linear segments.

Operation	Label	Formula
A distance between some point and an end point of the segment l	$D((x,y),l)$	$\min \{ ((x-x_1^l)^2 + (y-y_1^l)^2)^{1/2}, ((x-x_2^l)^2 + (y-y_2^l)^2)^{1/2} \}$
A distance between some point and a line containing the segment l	$d((x,y),l)$	$a^l x + b^l y + c^l$
An overlap between two segments l_1 and l_2 (where l_1 is longer than l_2):		*
The absolute overlap	$O(l_1,l_2)$	$\min \{ X_1 , L^{l1} \} - \max \{ 0, X_2 \}$
The relative overlap of a longer segment	$OL(l_1,l_2)$	$O(l_1,l_2) / L^{l_1}$
The relative overlap of a shorter segment	$OS(l_1,l_2)$	$O(l_1,l_2) / (X_2 - X_1)$
A distance between two segments	$D(l_1,l_2)$	$\min \{ d_1, d_2, d_3, d_4 \}$, where $d_1 = d((x_1^{l_1}, y_1^{l_1}), l_2)$, $d_2 = d((x_2^{l_1}, y_2^{l_1}), l_2)$, $d_3 = d((x_1^{l_2}, y_1^{l_2}), l_1)$, $d_4 = d((x_2^{l_2}, y_2^{l_2}), l_1)$
The point of intersection of lines containing two segments	$P(l_1,l_2)$	$\begin{bmatrix} x_0 \\ y_0 \end{bmatrix} = \begin{bmatrix} a^{l_1} & b^{l_1} \\ a^{l_2} & b^{l_2} \end{bmatrix}^{-1} \begin{bmatrix} -c^{l_1} \\ -c^{l_2} \end{bmatrix}$
A relative angle between two segments	$\alpha(l_1,l_2)$	$\alpha(l_1) - \alpha(l_2)$
An absolute angle between two segments	$\beta(l_1,l_2)$	**

* X_1, X_2 are the x-coordinates of the segment l_2 end points in a new coordinate system with the X-axis along the line l_1 and the origin in $(x_1^{l_1}, y_1^{l_1})$, rearranged so that $X_2 > X_1$

$$X_1 = - (x_1^{l_2} - x_1^{l_1}) b^{l_1} + (y_1^{l_2} - y_1^{l_1}) a^{l_1} \quad , \quad X_2 = - (x_2^{l_2} - x_1^{l_1}) b^{l_1} + (y_2^{l_2} - y_1^{l_1}) a^{l_1}$$

** The absolute angle if defined by the following way. Let i,j be indexes (i,j=1 or 2) for which the distance between $(x_i^{l_1}, y_i^{l_1})$ and $(x_j^{l_2}, y_j^{l_2})$ is a minimum. The absolute angle $\beta(l_1,l_2)$ between l_1 and l_2 is an angle between vectors $\mathbf{l_1^*}$ и $\mathbf{l_2^*}$ in counterclockwise, where

$$\mathbf{l_1^*} = \begin{bmatrix} x_{3-i}^{l_1} - x_i^{l_1} \\ y_{3-i}^{l_1} - y_i^{l_1} \end{bmatrix}, \quad \mathbf{l_2^*} = \begin{bmatrix} x_{3-i}^{l_2} - x_i^{l_2} \\ y_{3-i}^{l_2} - y_i^{l_2} \end{bmatrix}$$

Table 3. Perceptual relations between two linear segments.

Relation	Formula
Proximity(l_1,l_2)	$D(l_1,l_2) < D^*$
Collinear(l_1,l_2)	Proximity(l_1,l_2) and $\lvert \beta(l_1,l_2) - \pi \rvert < \Delta\alpha_1^*$ and $O(l_1,l_2) < \Delta O^*$
Parallel(l_1,l_2)	Proximity(l_1,l_2) and $\lvert\alpha(l_1,l_2)\rvert < \Delta\alpha_1^*$ and $\lvert\alpha(l_1,l_2) - \pi\rvert < \Delta\alpha_1^*$ and $\lvert\alpha(l_1,l_2) - 2\pi\rvert < \Delta\alpha_1$
Perpendicular(l_1,l_2)	Proximity(l_1,l_2) and ($\lvert \alpha(l_1,l_2) - \pi/2 \rvert < \Delta\alpha_2^*$ or $\lvert \alpha(l_1,l_2) - 3\pi/2 \rvert < \Delta\alpha_2^*$)
Corner(l_1,l_2)	Proximity(l_1,l_2) and not Parallel(l_1,l_2) and $D(P(l_1,l_2), l_1) < D_1^*$ and $D(P(l_1,l_2), l_2) < D_1^*$

Table 4. Model-based grouping of linear segments.

Model	Formula
Long Segment(l_1,l_2)	($D((x_1^{l_1},y_1^{l_1}),l_2)<d_{min}$ or $D((x_2^{l_1},y_2^{l_1}),l_2)<d_{min}$) and Collinear($l_1$,$l_2$)
Long Segment(l_1,...,l_n)	Parallel(l,l_i) and OS(l,l_i) > s and Collinear(l_i,l_j) , $i,j \in 1..n$
Parallel_Pair(l_1,l_2)	Parallel(l_1,l_2) and OL(l_1,l_2) > t_1 and OS(l_1,l_2) > t_2 and $D(l_1,l_2) > S_{min}$
U_Structure(l_1,l_2,l_3)	Parallel_Pair(l_1,l_2) and Corner(l_1,l_3) and Perpendicular(l_1,l_3) and $\lvert \beta(l_1,l_3) - \beta(l_3,l_1) \rvert < 2\Delta\alpha_2^*$
Rectangle(l_1,l_2,l_3,l_4)	U_Structure(l_1,l_2,l_3) and U_Structure(l_1,l_2,l_4) and $\lvert \beta(l_1,l_3) + \beta(l_1,l_4) - 2\pi \rvert < 2\Delta\alpha_2^*$
Ridge(l_1,l_2,l_3,l_4,l_5)	Rectangle(l_1,l_2,l_3,l_4) and Parallel(l_1,l_5) and Parallel(l_2,l_5) and $D(l_2,l_5) < D(l_1,l_2)$ And (OL(l_1,l_5) > s or OL(l_2,l_5) > s) and $D(l_1,l_5) < D(l_1,l_2)$

4 3D-RECONSTRUCTION THROUGH THE MATCHING IN OBJECT SPACE

The 3D-reconstruction of buildings is a next step after obtaining a building model from mono images. In dependence on problem one can use both method of exact reconstruction or method of approximate reconstruction.

For approximate reconstruction the building model extracted from mono image and the DEM are used. In this case an accuracy of reconstruction directly depends on an accuracy of the DEM. In this method the height of a building is taken directly from a DEM part inside an outline of a building (see Fig. 4a). The ground coordinates of linear segments are calculated by the least square method from ground coordinates of DSM nodes.

For an exact evaluation of 3D-coordinates of found models we use correlation-based matching in object space. The accuracy of obtained coordinates depends practically only on an accuracy of camera orientation parameters. Such accuracy can be sufficient for many applications, where the high-precision measurements of coordinates are required.

Let we have 2D segment l_S on the source image. We need to match 2D segment l_D on the destination image, that is we need to find l_D such that l_S and l_D are projections of one and the same 3D scene segment L on source and destination images respectively. To include a 3D-object model, we can require that there is parameterization ω of all possible L positions:

$$L = L(l_S, \omega),\ \omega \in \Omega \tag{1}$$

$$l_D = l_D(L) = l_D^*(l_S, \omega),\ \omega \in \Omega \tag{2}$$

Obviously, for matched 2D segments their one-sided vicinities on images must be similar. Note that one-sided vicinity usage is preferable due occlusions. Let V_S be vicinity of l_S and let V_D be appropriate vicinity of l_D. Note that dependence $V_D = V_D(V_S, \omega)$ includes 3D model of object facets. Thus, to match segments similarity of their one-sided vicinities as a function of ω should be maximized on the set Ω.

In our case of flat horizontal roof edges height coordinate H can be considered as parameter ω and bounds $H_{\min}$ and $H_{\max}$ define set Ω: $\Omega = [H_{\min}; H_{\max}]$. Under this assumption we consider facets of ridge roof model to be near horizontal. So (1) is a projective equation from image to object space; (2) is a collinearity equation from object space to image plane. The rough height range [H_{min}, H_{max}] can be computed from DEM as shown in Figure 4a. The maximum value is searched inside a building outline (black rectangle in Fig. 4a). In practice the value H_{max} is selected a little bit above obtained DEM value. The value H_{min} is searched in enough large area

around a building outline (white rectangle in Fig. 4a). Experimentally was found, that the minimum allowed DEM resolution is equal to half of minimum building width and further increase of DEM detail practically does not influence on matching results.

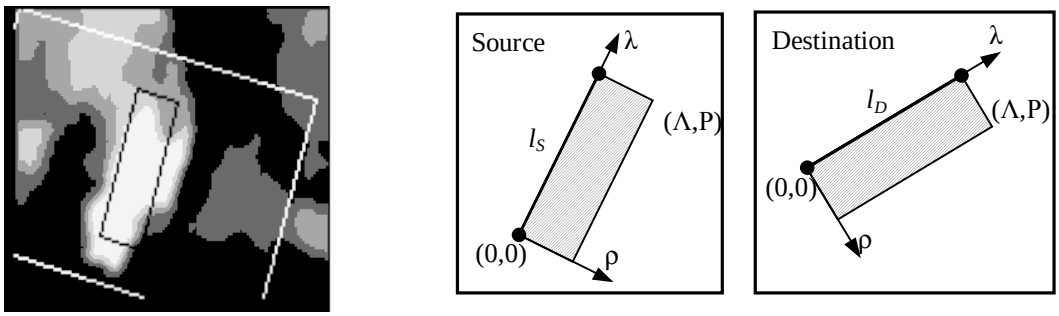

(a) (b)

Figure 4. Illustration of matching methods. (a) Height selection in accordance with building outline; (b) Vicinities used in precise 3D-reconstruction method.

To construct similarity measure let (λ, ρ) be a new image coordinate system as shown in Figure 4b. Here Λ is length of l_S in pixels and P is vicinity width in pixels. Then, the normalized correlation coefficient (3) of vicinities can be used.

$$corr(V_S, H) = \frac{\overline{S(\lambda,\rho)D(\lambda,\rho)} - \overline{S(\lambda,\rho)} \cdot \overline{D(\lambda,\rho)}}{\sqrt{\left[\overline{(S(\lambda,\rho))^2} - \overline{S(\lambda.\rho)}^2\right] \cdot \left[\overline{(D(\lambda,\rho))^2} - \overline{D(\lambda.\rho)}^2\right]}}, \quad (3)$$

where $S(\lambda,\rho) = S(x_S(\lambda,\rho), y_S(\lambda,\rho))$ is source image in new coordinates, $D(\lambda,\rho) = D(x_D(\lambda,\rho;\omega), y_D(\lambda,\rho;\omega))$ is destination image in new coordinates. Intensities in points with non-integer coordinates are obtained by bilinear interpolation.

The two-stage procedure of segment matching was developed. Both images of the stereopair are consequently used as the source ones. If matching results are coinciding for both stages then the pair of segments is accepted. If correlation value is less then some threshold (usually 0.3) then pair of segments is rejected. Example of matching of some segment pair is shown in Figure 5. It is visible that for both segments we obtain one and the same value of height: $H^* = 192\,\text{m}$. Figure 6 shows full result of segment matching for the test stereopair.

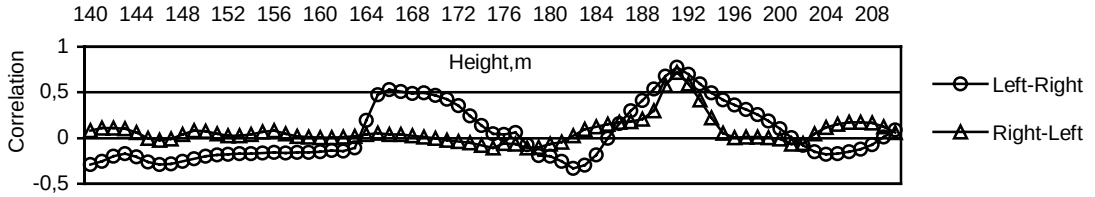

Figure 5. Correlation functions obtained during matching of some linear segment.

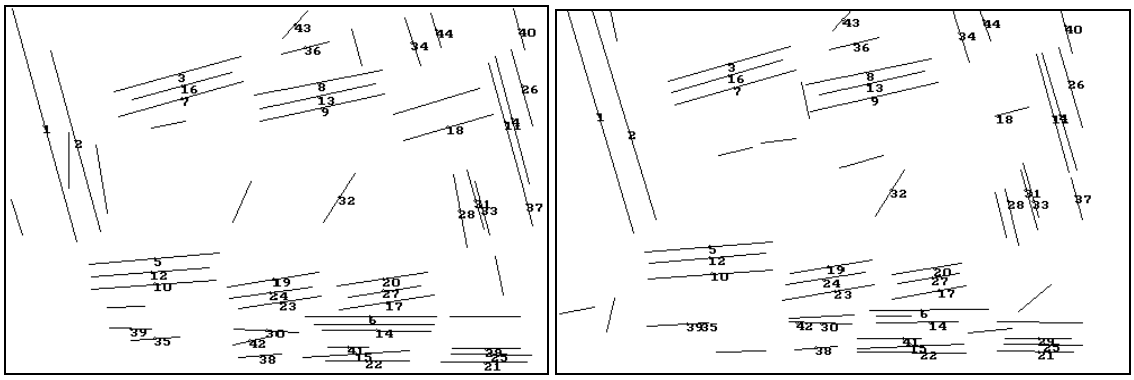

Figure 6. Full result of segment matching for test steropair. Left and right images (rotated versions) are shown. Correspondent numbers shows found matches.

5 ABOUT OTHER BUILDING MODELS

In the previous section our method of automatic extraction of rectangular buildings was reviewed. As the rectangular shape is one of the simplest models, it imposes strong constraints on building features. Due to such constraints and DEM support our method is able to extract considerable amount of distinct rectangular buildings on the images. The typical results of extraction are shown in Figure 7.

For each new model of objects different from rectangle it is necessary to design a new extraction algorithm. In GosNIIAS a number of the special projects on creation of 3D-models of man-made objects was made. Two examples of such projects are shown in Figures 8,9. The first example represents model of industrial plant with objects of the cylindrical shape (tank car of petroleum storage). For detection of circular objects the Hough transform was used. By this robust method 100% of objects were localized and extracted. The second example represents 3D-model of Great pyramids region in Giza, Cairo. For extraction of pyramid-shaped objects the modification of the reviewed algorithm of rectangular buildings extraction was used. The objects were extracted in a semi-automatic mode by single mouse click on one image near the pyramid top.

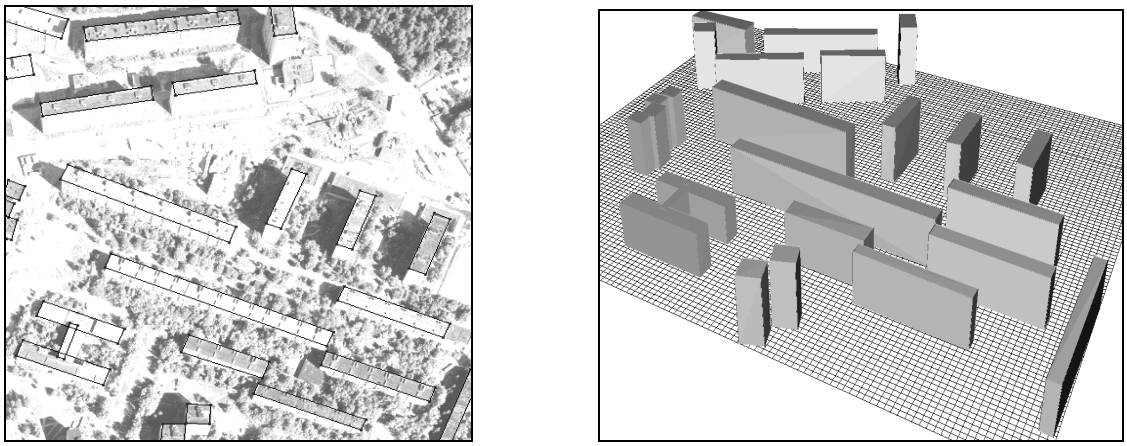

(a) (b)

Figure 7. Example of building extraction. (a) Left image of a stereopair; (b) 3D-view of extracted buildings. Some buildings (three complex ones at left side of view) were extracted in semi-automatic mode.

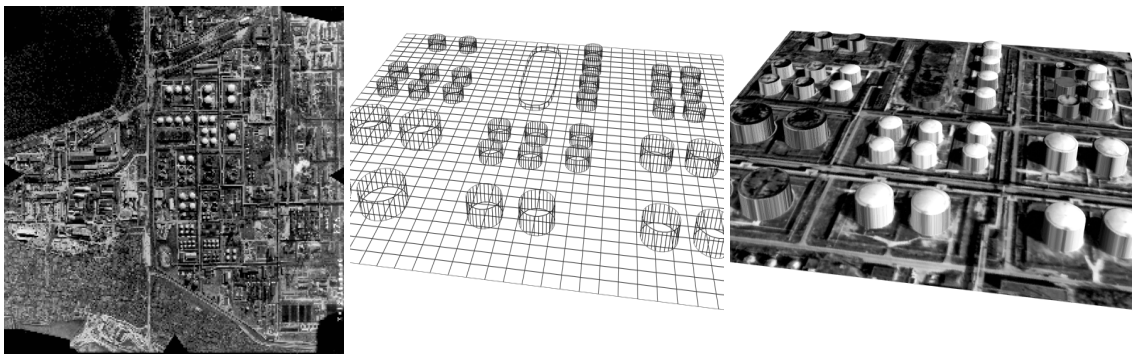

(a) (b) (c)

Figure 8. Example of man-made object extraction. (a) Original image (left image of a stereopair); (b) 3D-wireframe model obtained by Hough transform based extraction and stereo matching; (c) 3D site model.

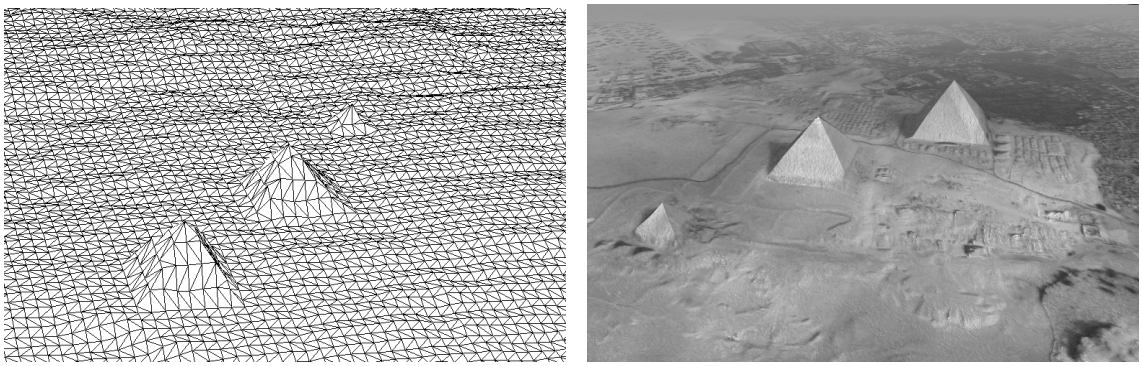

(a) (b)

Figure 9. Example of man-made object extraction. (a) 3D-wireframe model obtained by correlation based stereo matching and semi-automatic object extraction; (b) 3D site model.

6 SEMI-AUTOMATIC APPROACH

The new algorithm for more complex buildings extraction is developing which is now in at the state of semi-automatic algorithm. For maximum usage of already designed algorithm it is supposed, that the building models are composed from several rectangles.

In our semi-automatic approach user performs only supervisor functions, and the computer does all accurate operations. First of all user must select type of the roof model. As was mentioned above now we support only simplest models such as rectangle and ridge. The full model of a building can consist of any combination of these models. Then, user must mark on any image rough position of key points. Next, using marked positions of key points we can produce areas of interest on each available image. The key points extremely constrict area of interest and facilitate work of automatic part of the algorithm. Key point selection is some kind of "know how" and depends on building type. In case of rectangle flat roof two key points are used: one arbitrary point near each short side of the roof. Short sides itself are extracted by very sensitive method (Burns et al. 1986) in narrow areas near key points. Long sides are extracted by more stable Hough transform method, which is insensitive to line breaks (Fig. 10).

For Hough transform the following parameterization of straight line L is used:

$$L(\alpha, d) = \{ (x, y) \mid (x - x_0)\cos\alpha + (y - y_0)\sin\alpha \approx d \}, \quad (d, \alpha) \in [-d_{\max}; d_{\max}] \times [0; \pi), \qquad (4)$$

where (x_0,y_0) – is a center of the region of interest (ROI), defined by key points.

An accumulator array $H(\alpha,d)$ in our modification of Hough transform contains integral intensity step along straight line $L(d,\alpha)$ (see Bibitchev 2000):

$$H(\alpha, d) = \sum_{(x-x_0)\cos\alpha+(y-y_0)\sin\alpha\approx d} |\mathbf{g}(x, y)| \quad \exp\left[-\frac{\min^2\left\{|\alpha-\alpha_{\mathbf{g}}|, |\alpha-\alpha_{\mathbf{g}}+\pi|\right\}}{2\sigma_\alpha^2}\right] \tag{5}$$

In Equation 4, $\boldsymbol{g} = (g_x, g_y) = |\boldsymbol{g}|\ (\cos\alpha_g, \sin\alpha_g)$ is the gradient of image intensity. Along each line $L(\alpha,d)$ gradient magnitudes are summarized with weights depending on gradient direction. Gradient directions are supposed to be normally distributed with standard deviation σ_α.

Significant peaks in accumulator array are treated as straight lines. To detect significant peaks the method based on vertical and horizontal projections is used (Fig. 10b). Fist the vertical projection $Y(\alpha)$ of the accumulator array is calculated and global one-dimensional maxima α_{max} is searched for. Then the horizontal projection $X(d)$ is calculated in the narrow vertical strip corresponding to α_{max}. In $X(d)$ all one-dimensional local maxima $\{d_1, d_2, \ldots\}$ are extracted. Then subpixel positions of the straight lines are extracted from the array $H(\alpha,d)$ in the vicinities of the points $\{(\alpha_{max}, d_1), (\alpha_{max}, d_2), \ldots\}$.

In semi-automatic approach we do not need a DEM to determine areas of interest, because they can be determined more precisely by key points. To extract roof elevation we need special onground key points defined by user in one image. 3D coordinates of key points are determined by stereo correlation. In practice only one well-defined key point at building bottom are used. Thus, to extract whole building or part of more complex one only three key points are needed.

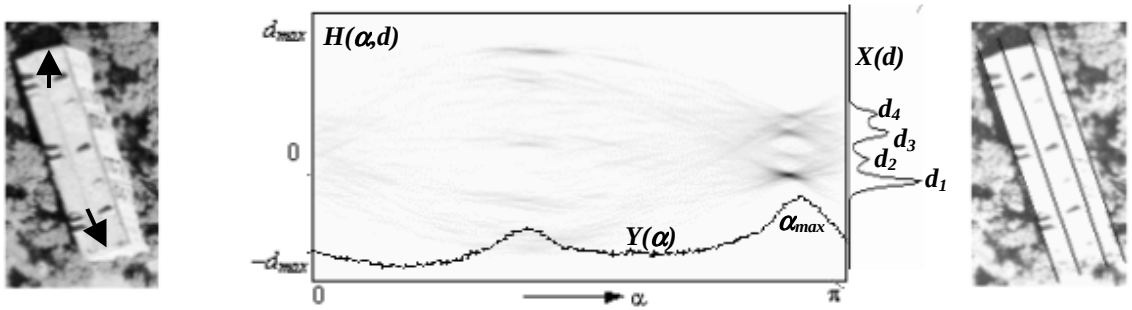

(a) (b) (c)

Figure 10. Extraction of long sides by Hough transform in semi-automatic approach. (a) Image ROI defined by key points (shown by arrows); (b) Illustration to projection-based detection of straight lines in accumulator array; (c) Long lines defined by significant peaks in accumulator array.

7 CONCLUSION

The purpose of the given work is technology of 3D-site model generation in PC-level computers. In this technology digital terrain models on large territory are created using Russian space images, and man-made objects and terrain models containing them are created using large-scale aerial images.

As a result of the research conducted in last years the following main results are obtained:

- the technology of generation of realistic 3D site models with man-made objects based on fusion different data sources (space and aerial images, DTMs, GIS data) is created;
- the methods of man-made objects extraction as a most important part of the technology were investigated;
- the effective automatic algorithms of extraction of objects with simple geometry based on grouping and stereo matching of straight lines were designed;
- semi-automatic algorithms based on approximate key points and modification of Hough transform are designed to extract more complex man-made objects.

REFERENCES

Bibitchev, A. 2000. Straight Edge Extraction from Multiple Views for Reconstruction of Man-Made Objects. *International Archives of Photogrammetry and Remote Sensing*, vol. 33, part B3, 71-78.

Burns, B., Hanson, A. & Risenman, E. 1986. Extracting Straight Lines. *Transactions PAMI* 8(2): 425-455.

Eckstein, W. 1996. Segmentation and Texture Analysis. *International Archives of Photogrammetry and Remote Sensing*, vol. 31, part B3, 65-75.

Haala, N. & Hahn, M. 1995. Data Fusion for the Detection and Reconstruction of Buildings. In A Gruen, O. Kuebler, P. Agouris (eds), *Automatic Extraction of Man-Maid Objects from Aerial and Space Images*: 211-220. Basel: Birkhauser Verlag.

Zheltov, S.U., Blokhinov, U.B., Stepanov, A.A., Sibiryakov, A.V. & Skryabin, S.V 1997. Computer 3D Site Model Generation Based on Aerial Images. *SPIE Proc. vol. 3084, 336-343*.